

## Pressure-induced valence change in $\text{YbAl}_3$ : A combined high-pressure inelastic x-ray scattering and theoretical investigation

Ravhi S. Kumar,<sup>1,\*</sup> Axel Svane,<sup>2</sup> G. Vaitheeswaran,<sup>3</sup> V. Kanchana,<sup>3</sup> Eric D. Bauer,<sup>4</sup> Michael Hu,<sup>5</sup> Malcolm F. Nicol,<sup>1</sup> and Andrew L. Cornelius<sup>1</sup>

<sup>1</sup>*Department of Physics and Astronomy and HiPSEC, University of Nevada, Las Vegas, Las Vegas, Nevada 89154, USA*

<sup>2</sup>*Department of Physics and Astronomy, University of Aarhus, DK-8000 Aarhus C, Denmark*

<sup>3</sup>*Division of Applied Materials Physics, Department of Materials Science and Engineering, Royal Institute of Technology, Brinellvägen 23, 100 44 Stockholm, Sweden*

<sup>4</sup>*Los Alamos National Laboratory, P.O. Box 1663, Los Alamos, New Mexico 87545, USA*

<sup>5</sup>*HPCAT, Carnegie Institution of Washington and Advanced Photon Source, Argonne National Laboratory, Argonne, Illinois 60439, USA*  
(Received 8 May 2008; revised manuscript received 16 July 2008; published 19 August 2008)

High-resolution x-ray-absorption (XAS) experiments in the partial fluorescence yield mode (PFY) and resonant inelastic x-ray emission (RXES) measurements were performed on the intermediate-valence compound  $\text{YbAl}_3$  under pressure of up to 38 GPa. The results of the  $\text{YbAl}_3$  PFY-XAS and RXES studies show that the valence of Yb increases smoothly from 2.75 at ambient pressure to 2.93 at 38 GPa. *In situ* angle-dispersive synchrotron high-pressure x-ray-diffraction experiments carried out using a diamond cell at room temperature show that the ambient pressure cubic phase is stable up to 40 GPa. The results obtained from self-interaction corrected local spin density-functional calculations to understand the pressure effect on the Yb valence and compressibility are in good agreement with the experimental results.

DOI: [10.1103/PhysRevB.78.075117](https://doi.org/10.1103/PhysRevB.78.075117)

PACS number(s): 71.20.Eh, 71.27.+a, 31.15.xw, 61.05.C-

### I. INTRODUCTION

Valence fluctuation is a phenomenon in many rare-earth and actinide systems, associated with heavy fermion behavior, the Kondo effect, unconventional superconductivity, and volume collapse transitions.<sup>1-4</sup> The effect arises because of strong intra-atomic correlations within the  $f$ -electron manifold, which enforces an atomlike or localized behavior, as opposed to the Bloch-type itinerant picture of electron waves appropriate for normal metallic states in solids. When two quasiautomatic configurations  $f^n$  and  $f^{n+1}$  become nearly degenerate as a consequence of the chemical environment, the interaction with the conduction electrons leads to a ground state given as a superposition of both configurations. A wealth of phenomena arises because of the interplay between the energy scales associated with Kondo coupling, the magnetic interatomic exchange interactions, and the crystal-field effects. The relative strengths of these energy scales may be varied by external parameters such as pressure.<sup>5-9</sup> Hence, high-pressure studies are powerful techniques for investigating valence fluctuation phenomena, which are the subject of the present work. Specifically, we explore by experiment and theory the valence fluctuating compound  $\text{YbAl}_3$  at high pressure.

$\text{YbAl}_3$  is an intermediate-valence compound and has a  $\text{CuAu}_3$ -type cubic structure. It exhibits a high Kondo temperature,  $T_K \sim 670$  K,<sup>10,11</sup> and has a magnetic susceptibility which follows a Curie-Weiss behavior above 250 K, corresponding to an effective magnetic moment of  $4.5\mu_B$ . This is indicative of fluctuating atomlike ( $\text{Yb} f^{13}$ ) local moments at high temperature due to charge distributions mainly centered at the Yb sites.<sup>12</sup> The electronic specific heat is large,  $58 \text{ mJ mol}^{-1} \text{ K}^{-2}$ .<sup>13</sup>  $\text{YbAl}_3$  finds application as a thermoelectric material with a large Seebeck coefficient of  $\sim -90 \mu\text{V K}^{-1}$  and a high electrical power factor.<sup>14</sup> Sev-

eral aspects of the low-temperature Fermi-liquid coherence and the crossover to the local-moment regime have been studied by transport,<sup>15</sup> inelastic nuclear scattering, and Lu substitution.<sup>16</sup> However, to extract direct information about the effective Yb valence, high-energy spectroscopic techniques, such as Mössbauer, x-ray-absorption, and high-resolution photoemission spectroscopy (PES) experiments, must be done.<sup>17-19</sup>

Recently, resonant inelastic x-ray emission (RXES) has emerged as an effective tool for probing mixed-valence systems, in which different valence transitions are selectively enhanced by choosing appropriate incident energies.<sup>20</sup> This technique in conjunction with pressure is an excellent method for studying the pressure-induced valence changes in rare-earth systems and has been applied to a variety of rare-earth intermetallic compounds in the past few years.<sup>21,22</sup> In this paper we describe an investigation of valence changes in  $\text{YbAl}_3$  using x-ray-absorption spectroscopy (XAS) in the partial fluorescence yield (PFY) mode as well as resonant inelastic x-ray emission studies performed up to 40 GPa. In addition we have measured high-pressure x-ray-diffraction patterns to determine the equation of state. Theoretical calculations have been carried out for  $\text{YbAl}_3$  using the self-interaction corrected local spin-density (SIC-LSD) method. This *ab initio* electronic structure method allows for an accurate, albeit approximate, description of the cohesive properties of the intermediate-valence state. The method has previously been applied for a range of Yb compounds, successfully accounting for the trends in observed Yb valences.<sup>23</sup>

The paper is organized as follows: In Sec. II we present our experimental and theoretical methodology, while results of experiment and theory are presented and discussed in Sec. III. Finally, Sec. IV concludes the present work.

## II. METHODS

### A. Experiment

Single crystals of  $\text{YbAl}_3$  crystals were grown in Al flux as described elsewhere.<sup>15</sup> The crystals were crushed into fine powder in an agate mortar. Powder x-ray-diffraction analysis revealed a single phase for the resultant product. The powdered sample was loaded with few tiny ruby chips and silicone fluid (polydimethylsiloxane) pressure transmitting medium into a 135- $\mu\text{m}$  hole drilled in a Be gasket. High pressures were generated using three UNLV-designed postpanoramic-type diamond anvil cells employing 300- $\mu\text{m}$  culet diamonds. The x-ray emission spectroscopic data were collected at Sector 16 ID-D of the Advanced Photon Source by focusing the incident x-ray beam to  $20 \times 50 \mu\text{m}^2$  (VH). The PFY and RXES experiments were performed at the Yb  $L_3$  absorption edge, where the signal from the sample was analyzed by a spherically bent Si single crystal and an Amptek detector in a Rowland circle. The total-energy resolution in our experiments is 1 eV.

High-pressure x-ray-diffraction experiments were performed at Sector 16 ID-B of the Advanced Photon Source in the angle-dispersive geometry. The sample was introduced into a 135- $\mu\text{m}$  hole of Re gasket preindented to 50  $\mu\text{m}$  with silicone fluid pressure medium and pressurized using a Mao-Bell-type diamond anvil cell.<sup>24</sup> Our earlier experiments showed that the hydrostaticity of the silicone fluid (1 cS) pressure medium used in the experiments behaves very similarly to argon at high-pressure range.<sup>25</sup> The pressure in the diamond cell was measured using ruby fluorescence technique. Diffraction images were collected using a MAR-345 imaging plate up to 40 GPa and integrated using the FIT2D software.<sup>26</sup> Further we have performed full structure refinement using the RIETVELD (REITICA) package.<sup>27</sup>

### B. Theory

The cohesive properties of  $\text{YbAl}_3$  are computed with the SIC-LSD approximation method.<sup>28–30</sup> This method is based on density-functional theory;<sup>31</sup> i.e., it relies on a total-energy functional by which the energy of the electron subsystem may be calculated at given nuclear positions. The single-electron states are determined from the solution of a Schrödinger equation with an effective potential which depends self-consistently on the total charge distribution in the solid. Compared to more conventional approaches, such as the LSD method, the SIC-LSD method includes a correction for the spurious self-interaction of individual electrons.<sup>30</sup> This term favors the formation of spatially localized states as compared to extended Bloch waves and provides a viable scheme for the calculation of the cohesive properties of rare-earth compounds.<sup>32,33</sup> In Yb compounds the method opens up the possibility of describing a mixed-valence state by either localizing all 14  $f$  electrons or localizing 13  $f$  electrons but allowing the 14th  $f$  electron to hybridize and form bands. The SIC-LSD method evaluates the total energy of the solid in both scenarios, and comparison establishes the appropriate ground-state configuration.<sup>23</sup> The divalent configuration of Yb is represented by localizing all 14  $f$  electrons in a closed shell, while the purely trivalent state occurs with 13 localized

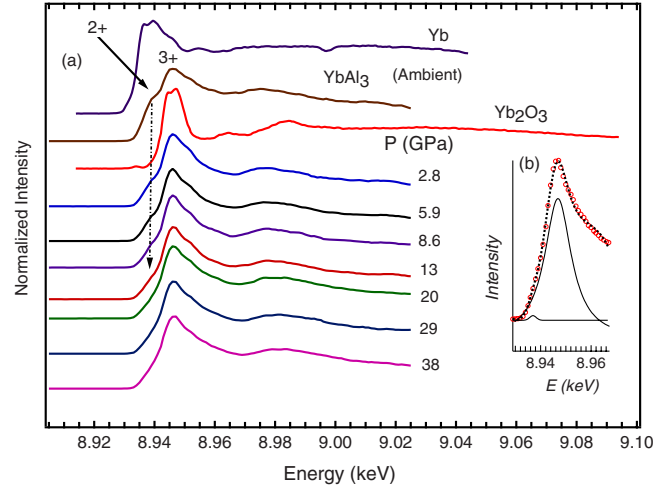


FIG. 1. (Color online) (a) X-ray-absorption spectra of  $\text{YbAl}_3$  in the PFY mode. The dotted arrow indicates the continuous decrease in the 2+ component as a function of pressure. The XAS spectrum of the  $\text{YbAl}_3$  sample at ambient temperature and pressure is shown with Yb and  $\text{Yb}_2\text{O}_3$  standards. (b) Decomposition of the 2+ and 3+ components (continuous lines) of the XAS spectrum at 38 GPa. The dotted line represents the fit and the open symbols represent the observed spectrum.

$f$  states in the case that the band of the 14th  $f$  electron is situated above the Fermi level. The effective valence of Yb in the intermediate-valence state follows from the degree of filling of the band of the 14th  $f$  electron. If the filling of the band is  $x$ , it implies that the wave function may be decomposed into an Yb  $f^{14}$  component with probability  $x$  and an Yb  $f^{13}$  component with probability  $1-x$ . Hence, this band filling is directly comparable to effective valences derived from experimental spectra, which involve distinct additive spectra from either of the two Yb configurations  $f^{13}$  and  $f^{14}$ , as is the case for XAS-PFY and RXES. Technical details of the present implementation can be found in Ref. 28.

## III. RESULTS AND DISCUSSION

### A. Partial fluorescence yield and resonant x-ray emission

The pressure dependence of the Yb  $L_3$  edge absorption data of  $\text{YbAl}_3$  up to 38 GPa is shown in Fig. 1. The spectral intensities of the 2+ and 3+ contributions at each pressure are calculated by assuming each spectrum as a combination of divalent and trivalent components. The line shape of the trivalent and divalent components was fitted as described elsewhere.<sup>34</sup> The PFY-XAS spectra of pure Yb metal and  $\text{Yb}_2\text{O}_3$  were collected at ambient conditions and served as standards for comparing the 2+ and 3+ intensities and line shapes. The Yb valence in  $\text{YbAl}_3$  at each pressure was estimated by substituting the integrated intensities of the 2+ and 3+ components at that pressure into the formula  $v = 2 + I_{3+}/(I_{2+} + I_{3+})$ , where  $I_{2+}$  and  $I_{3+}$  represent 2+ and 3+ intensities, respectively. On analyzing the PFY-XAS ambient spectrum of  $\text{YbAl}_3$ , we found that the 2+ component resonates at an incident energy  $E_{\text{in},2+} = 8.942$  keV and the 3+ component resonates at a little higher energy,  $E_{\text{in},3+}$

TABLE I. Estimated Yb valence in  $\text{YbAl}_3$  by various spectroscopic techniques such as PES, hard x-ray photoemission spectroscopy (HAXPES), and x-ray-absorption techniques.

| Pressure (GPa) | PFY-XAS <sup>a</sup> | RXES <sup>a</sup><br>( $E_{\text{in}}=8.938$ keV) | PES  | HAXPES                    | XAS                        | Theory <sup>a</sup> |
|----------------|----------------------|---|--|---------------------------|----------------------------|---------------------|
| Ambient        | 2.75                 | 2.76  | 2.65 (300 K) <sup>b</sup><br>2.65 (15 K) <sup>c</sup><br>2.74 (300 K) <sup>f</sup><br>2.77 (10 K) <sup>g</sup> | 2.71 (180 K) <sup>c</sup> | 2.775 (300 K) <sup>d</sup> | 2.62                |
| 9              | 2.82                 | 2.83  |  |                           |                            | 2.68                |
| 20             | 2.86                 | 2.85  |  |                           |                            | 2.72                |
| 38             | 2.93                 | 2.88  |  |                           |                            | 2.78                |

<sup>a</sup>Present work.<sup>b</sup>Reference 38.<sup>c</sup>Reference 39.<sup>d</sup>Reference 37.<sup>e</sup>Reference 40.<sup>f</sup>Reference 40.<sup>g</sup>Reference 11.

=8.950 keV. It is clearly seen that the divalent component, indicated by 2+ in Fig. 1, progressively decreases as pressure is increased.

The valence of Yb in  $\text{YbAl}_3$  has been studied by different techniques by various groups in the past two decades. While the electrical resistivity experiments performed earlier suggested that Yb possesses a nearly trivalent configuration,<sup>10</sup> Mössbauer experiments performed at 1.3–130 K showed no temperature dependence from the observed isomer shifts and the valence was reported as 2.7.<sup>18</sup> More experiments performed in later years provided further information about the intermediate valence and also its temperature dependence.<sup>11,35–37</sup> We have listed the valences estimated by different techniques in comparison with the current measurements and also listed the calculated valence of Yb at each increasing pressure by PFY-XAS and RXES in Table I. Even though the Anderson single impurity model reproduces the spectral features reported in the XAS and PES studies quite well, we notice that the valence reported strongly depends on the resolution and details of the spectral analysis. In most of the PES measurements, the Doniac-Sunjic line shapes were used to estimate the bulk features, and the surface contributions were fitted with Gaussian line shapes.<sup>11,40</sup>

High-pressure experiments involving the study of valence changes in the heavy fermion compounds are scarce. The mean valence of pure Yb metal was studied by high-pressure x-ray-absorption spectroscopy by Syassen *et al.*<sup>41</sup> up to 34 GPa. They reported a continuous valence change from the ambient divalent to the trivalent state above 30 GPa. The valence changes were associated with two structural phase transitions from fcc to bcc at 4 GPa and from a bcc to a hcp phase above 30 GPa. PFY-XAS and RXES experiments performed on  $\text{YbAl}_2$  recently showed pressure-induced valence change from 2.25 at ambient pressure to 2.9 at 38.5 GPa.<sup>34</sup> On comparing our PFY-XAS and RXES experimental results with these reports, we arrive at the following: The valence change in  $\text{YbAl}_3$  is sluggish compared to that in  $\text{YbAl}_2$  and is not associated with any structural phase transitions, as can

be seen from the diffraction results provided in Sec. III B. The RXES spectrum collected at 38 GPa is shown in Fig. 2. Inset (a) of the figure shows the pressure dependent RXES spectra excited with an incident energy  $E_{\text{in}}=8.938$  keV below the absorption threshold.

The increasing 3+ contribution is evident from the increase in the intensity of the peak around 8.950 keV, which is situated approximately 7 eV above the peak due to the 2+ component. Inset (b) of Fig. 2 shows the two-dimensional (2D) image of the RXES spectrum collected at ambient pressure. The branching of the 2+ and 3+ components is clearly visible. However, the valences estimated from the two measurements, i.e., PFY-XAS and RXES, differ at  $E_{\text{in}}=8.938$  keV as listed in Table I. This is due to the ambiguity

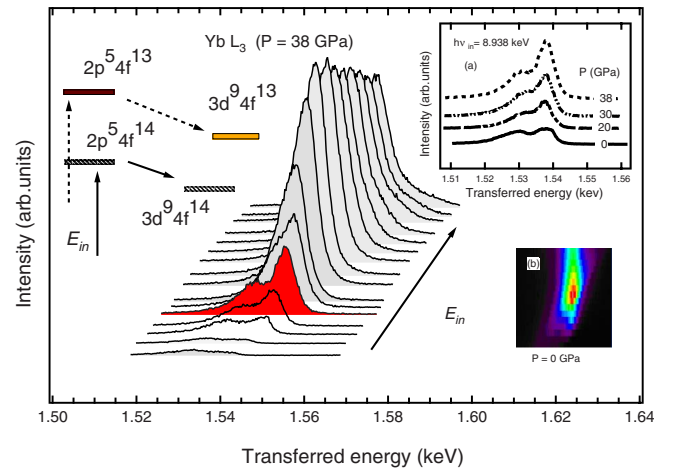


FIG. 2. (Color online) Resonant x-ray emission spectra of  $\text{YbAl}_3$  at 38 GPa. The incident energy was scanned in steps of 2 eV from 8.930 keV. A schematic representation of the transition is shown on the left. The RXES experiments were performed at the  $L_3$  edge of Yb by measuring the  $L\alpha_1$  x-ray emission as a function of pressure. (a) RXES spectrum with  $E_{\text{in}}=8.938$  keV at different pressures and (b) 2D image of the ambient spectrum.

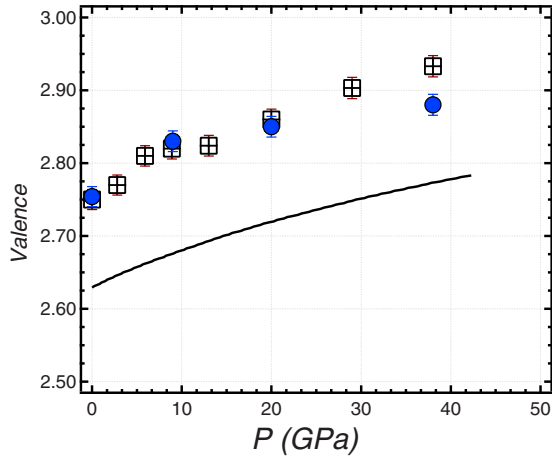


FIG. 3. (Color online) Valence as a function of pressure for PFY-XAS (squares) and RXES (circles) experiments. The solid line represents the theoretical simulation as discussed in Sec. III C.

in the intensity estimation for the fluorescent peak arising between the 2+ and the 3+ components as discussed previously for  $\text{YbAl}_2$ .<sup>34</sup> The pressure dependence of the Yb valence is illustrated in Fig. 3.

The effective valence determined from the SIC-LSD calculations is seen to be approximately 0.13 lower than the experimentally derived one. However the observed increase with pressure is well reproduced by the calculations. Given the intricacy of the concept of valence and the theoretical approximations of the SIC-LSD approach, the agreement can be considered quite satisfactory.

### B. High-pressure x-ray diffraction

Diffraction patterns collected at various pressures are shown in Fig. 4. The diffraction pattern collected at the lowest pressure ( $P=3.8$  GPa) in the diamond anvil cell was indexed well with the cubic  $Pm-3m$  structure as reported in the literature.<sup>42</sup> The prominent diffraction peaks were monitored on increasing pressure for any pressure-induced structural modifications. We have observed no changes in the diffraction pattern except a gradual shift in the diffraction lines as indicated by the dotted lines shown in the spectra.

No new features were observed in the diffraction patterns except a systematic shift of the lines during compression. The compound remained in the cubic structure up to the highest pressure achieved in our experiments. The bulk modulus was computed by fitting the pressure-volume data (Fig. 5) to a second-order Birch-Murnaghan equation of state. The values of  $B_0$  and  $B'_0$  are found to be  $B_0=65.2(3)$  and  $B'_0=5.6$ , respectively. The effect of high pressure on the crystal structure of rare-earth trialuminides was comprehensively investigated a long time ago.<sup>43</sup> Recently  $\text{RAl}_2$ - and  $\text{RAl}_3$ -type ( $R=\text{La}$  and  $\text{Ce}$ ) compounds have been studied under pressure up to 30 GPa.<sup>44</sup> The bulk modulus obtained for  $\text{YbAl}_3$  compares well with that of  $\text{YbAl}_2$ ,  $\text{LaAl}_3$ , and  $\text{CeAl}_3$  compounds as shown in Table II. However the bulk modulus of  $\text{YbAl}_3$  is found to be lower than the calculated bulk modulus values of similar transition-metal trialuminides such as

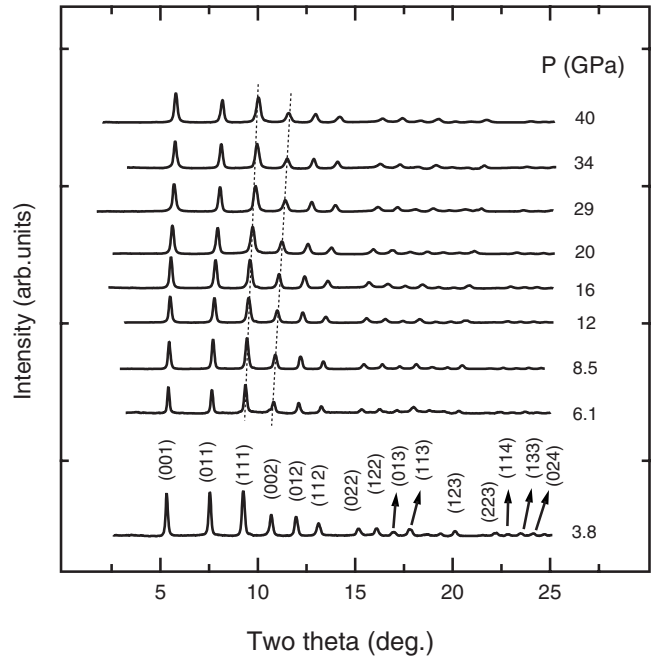


FIG. 4. Representative x-ray-diffraction patterns at different pressures for  $\text{YbAl}_3$ . The dotted lines are guides for the eye and indicate the shift observed in selected diffraction lines on increasing pressure. The patterns were collected using an incident x-ray wavelength of  $\lambda=0.3888$  Å.

$\text{ZrAl}_3$  and  $\text{HfAl}_3$ , which are used in high-temperature structural applications.<sup>45</sup>

### C. Results of calculations

The total energies of  $\text{YbAl}_3$  were calculated as a function of volume with the Yb localized configuration taken to be either  $f^{13}$  or  $f^{14}$ , as outlined in Sec. II B. The results are shown in Fig. 6. For the sampling of the charge density of

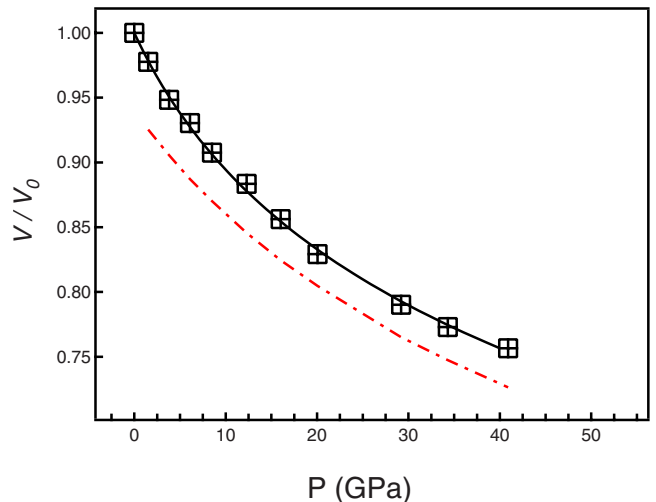


FIG. 5. (Color online) Pressure-volume relation of  $\text{YbAl}_3$ . The solid line is the fit with a second-order Birch-Murnaghan equation of state. The dotted line is the theoretical simulation. The estimated error bars lie within the size of the symbols.

TABLE II. Structural properties of YbAl<sub>3</sub> compared to those of CeAl<sub>3</sub> and LaAl<sub>3</sub>.

| Compound          | Ambient structure and cell parameters (Å) | Bulk modulus ( $B_0$ ) (GPa) | Pressure derivative ( $B'_0$ ) | Reference          |
|-------------------|---|------------------------------|--------------------------------|--------------------|
| YbAl <sub>3</sub> | Cubic, $Pm-3m$                            |                              |                                |                    |
|                   | $a=4.2125(2)$                             | 65.2(3)                      | 5.6                            | Expt. (this work)  |
|                   | $a=4.108$                                 | 92.3                         | 4.1                            | Theory (this work) |
| CeAl <sub>3</sub> | Hexagonal, $P6_3/mmc$                     |                              |                                |                    |
|                   | $a=6.541(5)$                              | 41(3)                        | 6.7                            | Ref. 44            |
|                   | $c=4.610(3)$                              |                              |                                |                    |
| LaAl <sub>3</sub> | Hexagonal, $P6_3/mmc$                     |                              |                                |                    |
|                   | $a=6.680(1)$                              | 63(4)                        | 4.0                            | Ref. 44            |
|                   | $c=4.619(1)$                              |                              |                                |                    |

the conduction electrons, the calculations used  $32^3$   $k$  points in the full Brillouin zone, corresponding to 969  $k$  points in the irreducible wedge of the Brillouin zone.

The theoretical ground state of YbAl<sub>3</sub> is found for the scenario with 13 localized  $f$  electrons, as explained in Sec. II B and the calculated intermediate-valence behavior agrees with the experimental observation. The total-energy minimum is found at a specific volume of  $490a_0^3$ , corresponding to a theoretical equilibrium lattice constant of 4.108 Å. This is 2.2% smaller than the experimental value of 4.2125(2) Å measured in the present work. This discrepancy is a combined effect of the underlying LSD approximation and the geometrical approximations of the present implementation of the SIC-LSD method. The LSD is well known to generally underestimate bond lengths.<sup>46</sup> The geometrical approximations of the present scheme involve the so-called atomic sphere approximation<sup>47</sup> (ASA), which in particular for Al is less accurate than a more complete full-potential treatment. For pure Al the lattice constant calculated with the restrictions of the ASA is 1.6% lower than the value calculated within a full-potential treatment. For Yb, on the other hand, the specific volume calculated within ASA is in perfect agreement with the experimental value.<sup>23</sup>

In Fig. 5 we compare the theoretical  $P(V)$  curve including this deficiency in equilibrium volume to the experimental

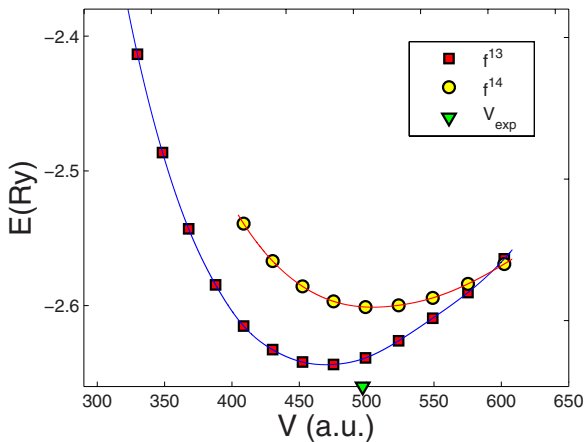


FIG. 6. (Color online) Total energy as a function of volume (per formula unit) for YbAl<sub>3</sub> calculated with the SIC-LSD approach with either 13 (squares) or 14 (circles) localized  $f$  electrons. The triangle marks the experimental equilibrium volume.

data. By coincidence, the equilibrium lattice constant for the divalent Yb configuration agrees better with the experimental value. However the energy of this state is found to be  $\sim 0.6$  eV higher than the intermediate-valence state (per formula unit); i.e., this configuration is not realizable.

The calculated bulk modulus of YbAl<sub>3</sub> is 92.3 GPa, which is considerably larger (by  $\sim 40\%$ ) than the experimental value of 65.2(3) GPa. The major reason for this is the smaller equilibrium volume discussed above, which also influences the curvature of the total-energy curve with an ensuing drastic influence on the bulk modulus. If evaluated at the experimental equilibrium volume, we find  $B(V_{\text{exp}})=77$  GPa,  $B'(V_{\text{exp}})=4.3$ , which are in considerably better agreement with the experimental values in Table II.

The calculated effective valence of Yb in YbAl<sub>3</sub> as a function of (calculated) pressure is included in Fig. 3 for comparison with the experimental values. The calculated values are seen to be somewhat smaller than the experimentally derived values by approximately 0.13. However they show

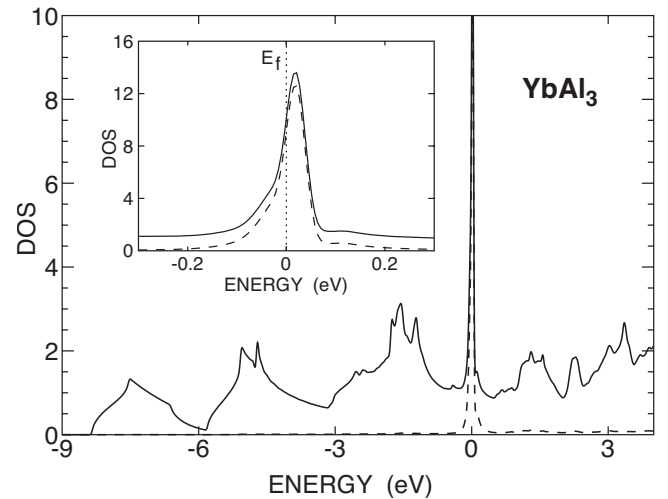


FIG. 7. SIC-LSD density of states (DOS) for YbAl<sub>3</sub> (units are states per formula unit and per eV). The Fermi energy is at zero energy. The full line is the total DOS, while the dashed line gives the Yb  $f$  projected DOS. The inset shows the region close to the Fermi level, where the partial occupation of the  $f$  resonance is evident. With pressure this resonance moves upward in energy with respect to the Al bands with an ensuing gradual depletion; i.e., Yb approaches the trivalent configuration.

the same smoothly increasing behavior with pressure. The effective valence increases by  $\sim 0.15$  as pressure is raised from 0 to 40 GPa, both in experiment and theory.

In Fig. 7, we show the density of one-electron states calculated for the intermediate-valence ground state of  $\text{YbAl}_3$ . One notices the Al valence bands ranging from 8.4 eV below the Fermi level and intersected by the narrow  $f$  band situated at the Fermi level. The inset shows the region close to the Fermi level and illustrates the partial filling of this band, which determines the effective valence. This density of states is not directly comparable to an experimental photoemission spectrum but merely serves to elucidate how the SIC-LSD ground state is built from one-particle states. Most notably, the localized states are not shown. A full treatment of photoemission in rare earths need to take into account the atomic character of the  $f$  electrons with all the multiplet effects of the initial and final states included.<sup>48</sup>

#### IV. CONCLUSIONS

We have studied the pressure dependence of the effective valence of Yb in the intermediate-valence compound  $\text{YbAl}_3$  using high-resolution PFY-XAS and RXES techniques. High-pressure spectra were collected up to 38 GPa. The equation of state of  $\text{YbAl}_3$  was also investigated up to 40 GPa using high-resolution powder x-ray diffraction. Self-

interaction corrected density-functional calculations were performed simultaneously in order to compare the experimental results. The pressure dependence of the Yb valence was derived from the experimental data and showed an increase from 2.75 to 2.93 as pressure is increased from 0 to 38 GPa. This trend compares well with the theoretical investigations.

#### ACKNOWLEDGMENTS

Work at HPCAT was supported by DOE Grant No. DEFG36-05GO08502. HPCAT is a collaboration among the UNLV High Pressure Science and Engineering Center, the Lawrence Livermore National Laboratory, the Geophysical Laboratory of the Carnegie Institution of Washington, and the University of Hawaii at Manoa. Work at Los Alamos was performed under the auspices of the U.S. DOE. The UNLV High Pressure Science and Engineering Center was supported by the U.S. Department of Energy, National Nuclear Security Administration, under Cooperative Agreement No. DE-FC08-01NV14049. The use of APS was supported by the U.S. Department of Energy, Office of Science, Office of Basic Energy Sciences, under Contract No. W-31-109-ENG-38. G.V. and V.K. acknowledge the Swedish Natural Science Foundation (VR) and Swedish Foundation for Strategic Research (SSF) for financial support.

\*ravhi@physics.unlv.edu

<sup>1</sup>A. C. Hewson, *The Kondo Problem to Heavy Fermions* (Cambridge University Press, Cambridge, England, 1993).

<sup>2</sup>J. M. Lawrence, P. S. Riseborough, and R. D. Park, *Rep. Prog. Phys.* **44**, 1 (1981).

<sup>3</sup>T. Kasuya and T. Saso, *Theory of Heavy Fermions and Valence Fluctuations* (Springer, Berlin, 1985).

<sup>4</sup>J. W. Allen, S. J. Oh, O. Gunnarsson, K. Schönhammer, M. B. Maple, M. S. Torikachvili, and I. Lindau, *Adv. Phys.* **35**, 275 (1986).

<sup>5</sup>E. D. Bauer, R. Hauser, E. Gratz, D. Gignoux, D. Schmitt, and J. Sereni, *J. Phys.: Condens. Matter* **4**, 7829 (1992).

<sup>6</sup>D. Wohlleben and B. Wittershagen, *Adv. Phys.* **34**, 403 (1985).

<sup>7</sup>Y. Kishimoto, Y. Kawasaki, and T. Ohno, *Phys. Lett. A* **317**, 308 (2003).

<sup>8</sup>A. V. Goltsev and M. M. Abd-Elmeguid, *J. Phys.: Condens. Matter* **17**, S813 (2005).

<sup>9</sup>P. Monachesi and A. Continenza, *Phys. Rev. B* **47**, 14622 (1993).

<sup>10</sup>E. E. Havinga, K. H. J. Buschow, and H. J. van Daal, *Solid State Commun.* **13**, 621 (1973).

<sup>11</sup>L. H. Tjeng, S.-J. Oh, E.-J. Cho, H.-J. Lin, C. T. Chen, G.-H. Gweon, J.-H. Park, J. W. Allen, T. Suzuki, M. S. Makivic, and D. L. Cox, *Phys. Rev. Lett.* **71**, 1419 (1993).

<sup>12</sup>K. H. J. Buschow, U. Goebel, and E. Dormann, *Phys. Status Solidi B* **93**, 607 (1979).

<sup>13</sup>T. Ebihara, S. Uji, C. Terakura, T. Terashima, E. Yamamoto, Y. Haga, Y. Inada, and Y. Onuki, *Physica B (Amsterdam)* **281-282**, 754 (2000).

<sup>14</sup>D. M. Rowe, V. L. Kuznetsov, L. A. Kuznetsova, and G. Min, *J. Phys. D* **35**, 2183 (2002).

<sup>15</sup>A. L. Cornelius, J. M. Lawrence, T. Ebihara, P. S. Riseborough, C. H. Booth, M. F. Hundley, P. G. Pagliuso, J. L. Sarrao, J. D. Thompson, M. H. Jung, A. H. Lacerda, and G. H. Kwei, *Phys. Rev. Lett.* **88**, 117201 (2002).

<sup>16</sup>E. D. Bauer, C. H. Booth, J. M. Lawrence, M. F. Hundley, J. L. Sarrao, J. D. Thompson, P. S. Riseborough, and T. Ebihara, *Phys. Rev. B* **69**, 125102 (2004); T. Ebihara, E. D. Bauer, A. L. Cornelius, J. M. Lawrence, N. Harrison, J. D. Thompson, J. L. Sarrao, M. F. Hundley, and S. Uji, *Phys. Rev. Lett.* **90**, 166404 (2003).

<sup>17</sup>F. Patthey, J. M. Imer, W. D. Schneider, Y. Baer, B. Delley, and F. Hulliger, *Phys. Rev. B* **36**, 7697 (1987).

<sup>18</sup>J. J. Joyce, A. B. Andrews, A. J. Arko, R. J. Bartlett, R. I. R. Blyth, C. G. Olson, P. J. Benning, P. C. Canfield, and D. M. Poirier, *Phys. Rev. B* **54**, 17515 (1996).

<sup>19</sup>J. W. Ross and E. Tronc, *J. Phys. F: Met. Phys.* **8**, 983 (1978).

<sup>20</sup>C. Dallera and M. Grioni, *Struct. Chem.* **14**, 57 (2003).

<sup>21</sup>C. Dallera, M. Grioni, A. Shukla, G. Vanko, J. L. Sarrao, J.-P. Rueff, and D. L. Cox, *Phys. Rev. Lett.* **88**, 196403 (2002).

<sup>22</sup>J.-P. Rueff, J.-P. Itie, M. Taguchi, C. F. Hague, J.-M. Mariot, R. Delaunay, J.-P. Kappler, and N. Jaouen, *Phys. Rev. Lett.* **96**, 237403 (2006).

<sup>23</sup>W. M. Temmerman, Z. Szotek, A. Svane, P. Strange, H. Winter, A. Delin, B. Johansson, O. Eriksson, L. Fast, and J. M. Wills, *Phys. Rev. Lett.* **83**, 3900 (1999); A. Svane, W. M. Temmerman, Z. Szotek, L. Petit, P. Strange, and H. Winter, *Phys. Rev. B* **62**, 13394 (2000).

- <sup>24</sup>H. K. Mao and P. M. Bell, *J. Geophys. Res.* **91**, 4673 (1986).
- <sup>25</sup>Y. Shen, Ravhi Kumar, Michael Pravica, and Malcolm Nicol, *Rev. Sci. Instrum.* **75**, 4450 (2004).
- <sup>26</sup>A. P. Hammersley, S. O. Svensson, M. Hanfland, A. N. Fitch, and D. Hausermann, *High Press. Res.* **29**, 301 (1996).
- <sup>27</sup>C. J. Howard and B. Hunter, *A Computer Program for Reitveld Analysis of X-ray and Neutron Powder Diffraction Patterns*, Lucas Height Research Laboratories, 1998 (unpublished).
- <sup>28</sup>A. Svane, *Phys. Rev. B* **53**, 4275 (1996).
- <sup>29</sup>W. M. Temmerman, A. Svane, Z. Szotek, H. Winter, and S. Beiden, in *Electronic Structure and Physical Properties of Solids: The Uses of the LMTO Method*, Lecture Notes in Physics Vol. 535, edited by H. Dreyse (Springer-Verlag, Berlin, 2000), pp. 286–312.
- <sup>30</sup>J. P. Perdew and A. Zunger, *Phys. Rev. B* **23**, 5048 (1981).
- <sup>31</sup>P. Hohenberg and W. Kohn, *Phys. Rev.* **136**, B864 (1964).
- <sup>32</sup>P. Strange, A. Svane, W. M. Timmerman, Z. Szotek, and H. Winter, *Nature (London)* **399**, 756 (1999).
- <sup>33</sup>A. Svane, W. M. Temmerman, Z. Szotek, L. Petit, P. Strange, and H. Winter, *Phys. Rev. B* **62**, 13394 (2000); G. Vaitheeswaran, L. Petit, A. Svane, V. Kanchana, and M. Rajagopalan, *J. Phys. C* **16**, 4429 (2004); A. Svane, V. Kanchana, G. Vaitheeswaran, G. Santi, W. M. Temmerman, Z. Szotek, P. Strange, and L. Petit, *Phys. Rev. B* **71**, 045119 (2005); A. Svane, G. Santi, Z. Szotek, W. M. Temmerman, P. Strange, M. Horne, G. Vaitheeswaran, V. Kanchana, and L. Petit, *Phys. Status Solidi B* **241**, 3185 (2004).
- <sup>34</sup>C. Dallera, E. Annese, J.-P. Rueff, A. Palenzona, A. Vanko, L. Braicovich, A. Shukla, and M. Grioni, *Phys. Rev. B* **68**, 245114 (2003).
- <sup>35</sup>E.-J. Cho, S.-J. Cho, C. G. Olson, J.-S. Kang, R. O. Anderson, L. Z. Liu, J. H. Park, and J. W. Allen, *Physica B (Amsterdam)* **186-188**, 70 (1993).
- <sup>36</sup>S. Suga, A. Sekiyama, S. Imada, A. Shigemoto, A. Yamasaki, M. Tsunekawa, C. Dallera, L. Braicovich, T.-L. Lee, O. Sakai, T. Ebihara, and Y. Onuki, *J. Phys. Soc. Jpn.* **74**, 2880 (2005).
- <sup>37</sup>J. M. Lawrence, G. H. Kwei, P. C. Canfield, J. G. DeWitt, and A. C. Lawson, *Phys. Rev. B* **49**, 1627 (1994).
- <sup>38</sup>E. J. Cho, J. S. Chung, S. J. Oh, S. Suga, M. Taniguchi, A. Kakizaki, A. Fujimori, H. Kato, T. Miyahara, T. Suzuki, and T. Kasuya, *Phys. Rev. B* **47**, 3933 (1993).
- <sup>39</sup>A. Sekiyama and S. Suga, *J. Electron Spectrosc. Relat. Phenom.* **137-140**, 681 (2004).
- <sup>40</sup>S.-J. Oh, *Physica B (Amsterdam)* **186-188**, 26 (1993).
- <sup>41</sup>K. Syassen, G. Wortmann, J. Feldhaus, K. H. Frank, and G. Kaindl, *Phys. Rev. B* **26**, 4745 (1982).
- <sup>42</sup>A. Palenzona, *J. Less-Common Met.* **29**, 289 (1972).
- <sup>43</sup>J. F. Cannon and H. Tracy Hall, *J. Less-Common Met.* **40**, 313 (1975).
- <sup>44</sup>M. Sekar, N. V. Chandra Shekar, P. Ch. Sahu, N. R. Sanjay Kumar, and K. Govinda Rajan, *Physica B (Amsterdam)* **324**, 240 (2002).
- <sup>45</sup>C. Colinet and A. Pasturel, *J. Alloys Compd.* **319**, 154 (2001).
- <sup>46</sup>R. O. Jones and O. Gunnarsson, *Rev. Mod. Phys.* **61**, 689 (1989).
- <sup>47</sup>O. K. Andersen, *Phys. Rev. B* **12**, 3060 (1975).
- <sup>48</sup>S. Lebegue, G. Santi, A. Svane, O. Bengone, M. I. Katsnelson, A. I. Lichtenstein, and O. Eriksson, *Phys. Rev. B* **72**, 245102 (2005).